Substituent Effects on ^{103}Rh NMR Chemical Shifts and Reactivities. A Density Functional Study

Michael Bühl†

Organisch-chemisches Institut, Universität Zürich, Winterthurerstrasse 192, CH-8057 Zürich, Switzerland

Received July 24, 1996⊗

^{103}Rh chemical shifts, computed using the SOS-DFPT approach (sum-over-states density functional perturbation theory), large basis sets, and optimized geometries, correlate well with the corresponding experimental data for $[Rh(C_5H_5)_2]^+$, $[Rh(CO)_2(C_5H_4X)]$ (X = H, NMe_2, Cl, NO_2), $[Rh(CO)_4]^-$, $[RhCl_2(CO)_2]^-$, and [Rh(acac)L_2] (acac = acetylacetonato, L_2 = $(C_2H_4)_2$, 1,5-cyclooctadiene, cyclooctatetraene). The slope of the regression line, however, is only ca. 0.8 instead of unity. Scaled appropriately, the theoretical $\delta(^{103}Rh)$ values differ from experiment by less than 100 ppm (mean absolute deviation), over a range of 3600 ppm. In the $[Rh(CO)_2(C_5H_4X)]$ series, the computed activation barriers of PH_3 addition correlate well with the experimental rate constants for CO/PPh_3 displacement, thereby reproducing theoretically the relation between reactivities and ^{103}Rh chemical shifts that has been reported experimentally.

Introduction

There is no immediate, general relation between chemical shifts and kinetic parameters, yet a number of such correlations have been established for systems involving transition-metal complexes.[1−7] The potential of these correlations is that reactivities and, in some cases, even catalytic activities[3,7] of a given compound can be estimated from its NMR spectrum alone. For instance, in the system shown by eq 1, the $\delta(^{103}Rh)$ data

$$[Rh(CO)_2(C_5H_4X)] + PR_3 \rightarrow [Rh(PR_3)(CO)(C_5H_4X)] + CO \quad (1)$$

for the reactants have been found to correlate linearly with the logarithm of the observed rate constant for CO/PPh_3 displacement (R = C_5H_6, X = H, CH_3, NMe_2, CF_3, Cl, NO_2).[5] In order to test if theory can reproduce and, possibly, help to rationalize these findings, a study of this reaction is now reported employing the tools of modern density functional theory (DFT).[8,9] Special attention is called to the chemical shifts of the transition metal, the accurate calculation of which remains a challenge for theory.

Most transition-metal complexes are not well described by standard Hartree−Fock SCF (self-consistent field) wave functions; highly sophisticated, electron-correlated ab initio methods are required[10−12] which are in many cases prohibitively expensive. DFT-based methods offer promising alternatives for the computations of both energetics[13] and magnetic properties[14−17] of these systems, and the number of DFT studies of transition-metal compounds and their reactions is increasing rapidly.[18−21] On the NMR side, extensive studies by Kaupp and by others have demonstrated that the experimental chemical shifts of ligands in the coordination sphere of transition metals can be reliably reproduced employing DFT-based methods,[22−28] for instance with SOS-DFPT (sum-over-states density functional perturbation theory).[14,15]

Somewhat disappointingly, the same approach does not work as satisfactorily in the case of ^{57}Fe chemical shifts: computed and experimental chemical shifts have been shown to correlate, but only with a slope of 0.55

† E-mail: buehl@oci.unizh.ch.

⊗ Abstract published in *Advance ACS Abstracts,* December 15, 1996.

(1) Meier, E. J.; Kozminski, W.; Linden, A.; Lustenberger, P.; von Philipsborn, W. *Organometallics* **1996**, *15*, 2469.
(2) Tedesco, V.; von Philipsborn, W. *Organometallics* **1995**, *14*, 3600.
(3) (a) Fornica, R.; Görls, H.; Seeman, B.; Leitner, W. *J. Chem. Soc., Chem. Commun.* **1995**, 1479. (b) Angermund, K.; Baumann, W.; Dinjus, E.; Fornika, R.; Görls, H.; Kessler, M.; Krüger, C.; Leitner, W.; Lutz, F. *Chem. Eur. J.*, in press.
(4) Koller, M. Ph.D. Thesis, University of Zürich, 1993.
(5) Koller, M.; von Philipsborn, W. *Organometallics* **1992**, *11*, 467.
(6) DeShong, P.; Sidler, D. R.; Rybczynski, P. J.; Ogilvie, A. A.; von Philipsborn, W. *J. Org. Chem.* **1989**, *54*, 5432.
(7) Bönnemann, H.; Brijoux, W.; Brinkmann, R.; Meurers, W.; Mynott, R.; von Philipsborn, W.; Egolf, T. *J. Organomet. Chem.* **1984**, *272*, 231.
(8) Seminario, J. M., Politzer, P., Eds. *Modern Density Functional Theory*; Elsevier: Amsterdam, 1995.
(9) Parr, R. G.; Yang, W. *Density Functional Theory of Atoms and Molecules*, Academic Press: Oxford, U.K., 1989.
(10) E.g.: Siegbahn, P. E. M. *J. Am. Chem. Soc.* **1996**, *118*, 1487.
(11) Frenking, G.; Antes, I.; Böhme, M.; Dapprich, S.; Ehlers, A. W.; Jonas, V.; Neuhaus, A.; Otto, M.; Stegmann, R.; Veldkamp, A.; Vyboishchikov, S. F. In *Reviews in Computational Chemistry;* Lipkowitz, K. B., Boyd, D. B., Eds.; VCH: New York, 1996; Vol. 8, p 63.
(12) Review: Veillard, A. *Chem. Rev.* **1991**, *91*, 743.
(13) Review: Ziegler, T. *Chem. Rev.* **1991**, 91, 651; *Can. J. Chem.* **1995**, *73*, 743.
(14) Malkin, V. G.; Malkina, O. L.; Casida, M. E.; Salahub, D. R. *J. Am. Chem. Soc.* **1994**, *116*, 5898.
(15) Malkin, V. G.; Malkina, O. L.; Eriksson, L. A.; Salahub, D. R. In *Modern Density Functional Theory*; Seminario, J. M., Politzer, P., Eds.; Elsevier: Amsterdam, 1995; p 273.
(16) Schreckenbach, G.; Ziegler, T. *J. Chem. Phys.* **1995**, *99*, 606.
(17) Lee, A. M.; Handy, N. C.; Colwell, S. M. *J. Chem. Phys.* **1995**, *103*, 10095.
(18) For some recent examples, see e.g.: Margl, P.; Lohrenz, J. C. W.; Ziegler, T.; Blöchl, P. E. *J. Am. Chem. Soc.* **1996**, *118*, 4434.
(19) Margl, P.; Ziegler, T.; Blöchl, P. E. *J. Am. Chem. Soc.* **1996**, *118*, 5412.
(20) Solà, M.; Ziegler, T. *Organometallics* **1996**, *15*, 2611.
(21) Holthausen, M. C.; Fiedler, A.; Schwarz, H.; Koch, W. *Angew. Chem., Int. Ed. Engl.* **1995**, *34*, 2282.
(22) Kaupp, M. *J. Chem. Soc., Chem. Commun.* **1996**, 1141.
(23) Kaupp, M. *Chem. Ber.* **1996**, *129*, 527.
(24) Kaupp, M. *Chem. Eur. J.* **1996**, *2*, 194.
(25) Kaupp, M.; Malkin, V. G.; Malkina, O. L.; Salahub, D. R. *Chem. Eur. J.* **1996**, *2*, 24.
(26) Kaupp, M.; Malkin, V. G.; Malkina, O. L.; Salahub, D. R. *J. Am. Chem. Soc.* **1995**, *117*, 1851.
(27) Kaupp, M.; Malkin, V. G.; Malkina, O. L.; Salahub, D. R. *Chem. Phys. Lett.* **1995**, *235*, 382.
(28) Ruiz-Morales, Y.; Schreckenbach, G.; Ziegler, T. *J. Phys. Chem.* **1996**, *100*, 3359.

S0276-7333(96)00615-2 CCC: $14.00

instead of unity for the corresponding regression lines.[29] There are indications from conventional ab initio methods that the description of compounds of the heavier (4d and 5d) transition metals often requires somewhat less sophisticated, correlated wave functions than their lighter counterparts from the first transition row.[11] It thus seemed possible that ^{103}Rh chemical shifts might be better described with the SOS-DFPT approach than the $\delta(^{57}\mathrm{Fe})$ values mentioned above. A representative set of organorhodium compounds has therefore been studied comprising low-valent cyclopentadienyl, CO, and olefin complexes which span a $\delta(^{103}\mathrm{Rh})$ range of ca. 3600 ppm.

Computational Details

Geometries have been fully optimized without symmetry constraints (except where otherwise noted) with the Gaussian 94 package[30] employing the gradient-corrected exchange-correlation functionals of Becke (1988)[31] and Perdew (1986),[32] together with a quasi-relativistic effective core potential and the corresponding [6s5p3d] valence basis set for Rh[33] and standard 6-31G* basis[34] on the ligands (designated BP86/ECP1). Geometries and vibrational frequencies of a number of transition-metal carbonyls have been shown to agree very well with the experimental data at that level.[35] For each of the substituted species **2b**−**d**, several conformations of the C_5H_4X ligand with respect to the $Rh(CO)_2$ moiety had initially been optimized at the SCF/ECP1 level, followed by reoptimization of the most stable of each conformer at BP86/ECP1.

Magnetic shielding tensors have been computed for the BP86/ECP1 geometries employing the SOS-DFPT method[14,15] in its LOC1 approximation with the IGLO (individual gauge for localized orbitals)[36−38] choice of gauge origins, as implemented in the deMon[39,40] program, employing the 1991 exchange-correlation functional of Perdew and Wang (designated PW91).[41,42] A fine integration grid (FINE option) has been used, together with the uncontracted [26s16p13d] basis of Partridge and Faegri for Rh[43] (i.e. the 25s15p12d set augmented by one s, p, and d set each, with the exponents of the additional functions obtained by division by 2.5 of the most diffuse AO coefficients) and IGLO basis II[38] for the ligands (which is essentially of polarized triple-ζ quality), designated SOS-DFPT/IIa. Auxiliary basis sets of the type (5,5) for Rh, (5,4) for Cl, (5,2) for C, N, and O, and (5,1) for H have been used for the fit of the exchange-correlation potential and of the charge densities (*n*,*m* stands for *n* s functions and *m* spd shells). For the ligands, basis II and auxiliary basis sets are the same as have been used in the $\delta(^{13}\mathrm{C})$ and $\delta(^{17}\mathrm{O})$ computations of transition-metal complexes.[22−27] For comparison, magnetic shieldings have also been computed with the conventional GIAO-SCF method,[44,45] as implemented[46] in the TURBOMOLE[47] package, employing the same basis set and geometries. In addition, SOS-DFPT chemical shifts have been computed using basis II, i.e. the same basis II for the ligands, but with a somewhat smaller, well-tempered [16s10p9d] basis[48] on Rh (contracted from the 22s14p12d set and augmented with two d shells of the well-tempered series).

In the experiments, $\delta(^{103}\mathrm{Rh})$ data are given relative to a standard frequency of $\Xi = 3.16$ MHz (with $\delta(^1\mathrm{H})$ of $SiMe_4$ at 100 MHz).[49,50] The magnetic shieldings corresponding to δ 0, σ(standard), have been evaluated as the intercepts of the σ(calcd) vs. δ(exptl) linear regressions (see Table 1 for the values), and theoretical relative shifts have been calculated as $\delta = \sigma(\mathrm{standard}) - \sigma(\mathrm{calcd})$. The scale factors for the SOS-DFPT/IIa chemical shifts have been taken as 1.28, i.e. the reciprocal slope of the σ(calcd)/δ(expt) regression. For selected compounds, additional SOS-DFPT calculations have been performed using a larger basis set on the ligands (IGLO basis III[38] instead of II) or using other local (Vosko, Wilk, and Nusair, designated VWN)[51] or nonlocal (Becke)[31] functionals.

For the parent substitution reaction (1) (X, R = H), the nature of each stationary point has been verified by numerical frequency calculations at the BP86/ECP1 level. With the transition state **IIa(TS)** as the starting point, the intrinsic reaction coordinate[52] has been followed to the intermediate **IIa** and toward further dissociation of PH_3, in order to ensure that the correct transition structure had been located. Single-point energy calculations have been performed for the BP86/ECP1 geometries using the same ECP1 basis and other combinations of functionals, namely nonlocal VWN, Becke (1988) and PW91 (designated BPW91), or Becke's three-parameter DFT/Hartree−Fock hybrid functional[53] together with the correlation functional of Lee, Yang, and Parr[54] (designated B3LYP).

For the search of the substituted transition structures, single-point BP86/ECP1 calculations had first been performed for various rotamers, i.e. for the parent structure **IIa(TS)** with every single of the hydrogen atoms replaced by NH_2 (results not reported), Cl, or NO_2. In each case, the isomers with the substituents attached to the uncoordinated double bond (cf. Figure 4) were more stable than the other ones by at least 2 kcal/mol and have subsequently been subject to full transition state optimizations. The search for **IIb(TS)** started from the optimized transition structure for $X = NH_2$ with the two amino hydrogens replaced by CH_3. No frequencies have been computed for the stationary points located, but the eigenvectors of the single, negative eigenvalue of the Hessian have been basically the same as for the parent **IIa(TS)** in each case.

Results and Discussion

1. Chemical Shifts. The BP86/ECP1 geometries of compounds **1**−**5** are displayed in Figure 1, together with

(29) Bühl, M.; Malkina, O. L.; Malkin, V. G. *Helv. Chim. Acta* **1996**, *79*, 742.
(30) Frisch, M. J.; Trucks, G. W.; Schlegel, H. B.; Gill, P. M. W.; Johnson, B. G.; Robb, M. A.; Cheeseman, J. R.; Keith, T.; Petersson, G. A.; Montgomery, J. A.; Raghavachari, K.; Al-Laham, M. A.; Zakrzewski, V. G.; Ortiz, J. V.; Foresman, J. B.; Peng, C. Y.; Ayala, P. Y.; Chen, W.; Wong, M. W.; Andres, J. L.; Replogle, E. S.; Gomperts, R.; Martin, R. L.; Fox, D. J.; Binkley, J. S.; DeFrees, D. J.; Baker, J.; Stewart, J. J. P.; Head-Gordon, M.; Gonzales, C.; Pople, J. A. Gaussian 94; Gaussian, Inc., Pittsburgh, PA, 1995.
(31) Becke, A. D. *Phys. Rev. A* **1988**, *38*, 3098.
(32) Perdew, J. P. *Phys. Rev. B* **1986**, *33*, 8822; **1986**, *34*, 7406.
(33) Andrae, D.; Häussermann, U.; Dolg, M.; Stoll, H.; Preuss, H., *Theor. Chim. Acta* **1990**, *77*, 123.
(34) Hehre, W. J.; Radom, L.; Schleyer, P. v. R.; Pople, J. A. *Ab initio Molecular Orbital Theory*; Wiley: New York, 1986.
(35) Jonas, V.; Thiel, W. *J. Chem. Phys.* **1995**, *102*, 8474.
(36) Kutzelnigg, W. *Isr. J. Chem.* **1980**, *19*, 193.
(37) Schindler, M.; Kutzelnigg, W. *J. Chem. Phys.* **1982**, *76*, 1919.
(38) Kutzelnigg, W.; Fleischer, U.; Schindler, M. In *NMR Basic Principles and Progress*; Springer-Verlag: Berlin, 1990; Vol. 23, p 165.
(39) Salahub, D. R.; Fournier, R.; Mlynarski, P.; Papai, I.; St-Amant, A.; Ushio, J. In *Density Functional Methods in Chemistry*; Labanowski, J. K., Andzelm, J. W., Eds.; Springer: New York, 1991; p 77.
(40) St-Amant, A.; Salahub, D. R. *Chem. Phys. Lett.* **1990**, *169*, 387.
(41) Perdew, J. P.; Wang, Y. *Phys. Rev. B* **1992**, *45*, 13244.
(42) Perdew, J. J. In *Electronic Structure of Solids*; Ziesche, P., Eischrig, H., Eds.; Akademie Verlag: Berlin, 1991.
(43) Partridge, H.; Faegri, K. *Theor. Chim. Acta* **1992**, *82*, 207.
(44) Ditchfield, R. *Mol. Phys.* **1974**, *27*, 789.
(45) Wolinski, K.; Hinton, J. F.; Pulay, P. *J. Am. Chem. Soc.* **1990**, *112*, 8251.
(46) Häser, M.; Ahlrichs, R.; Baron, H. P.; Weis, P.; Horn, H. *Theor. Chim. Acta* **1992**, *83*, 455.
(47) Ahlrichs, R.; Bär, M.; Häser, M.; Horn, H.; Kölmel, C. *Chem. Phys. Lett.* **1989**, *162*, 165.
(48) Huzinaga, S.; Klobukowski, M. *J. Mol. Struct.* **1988**, *167*, 1.
(49) Benn, R.; Rufinska, A. *Angew. Chem., Int. Ed. Engl.* **1986**, *25*, 861.
(50) (a) Mann, B. E. In *Transition Metal Nuclear Magnetic Resonance*; Pregosin, P. S., Ed.; Elsevier: Amsterdam, 1991; p 77. (b) Mann, B. E. In *NMR of Newly Accessible Nuclei*; Laszlo, P., Ed.; Academic Press: New York, 1983; p 301.
(51) Vosko, S. H.; Wilk, L.; Nusair, M. *Can. J. Phys.* **1980**, *58*, 1200.
(52) Gonzales, C.; Schlegel, H. B. *J. Chem. Phys.* **1989**, 90, 2154; **1990**, *94*, 5523.
(53) Becke, A. D. *J. Chem. Phys.* **1993**, *98*, 5648.
(54) Lee, C.; Yang, W.; Parr, R. G. *Phys. Rev. B* **1988**, *37*, 785.

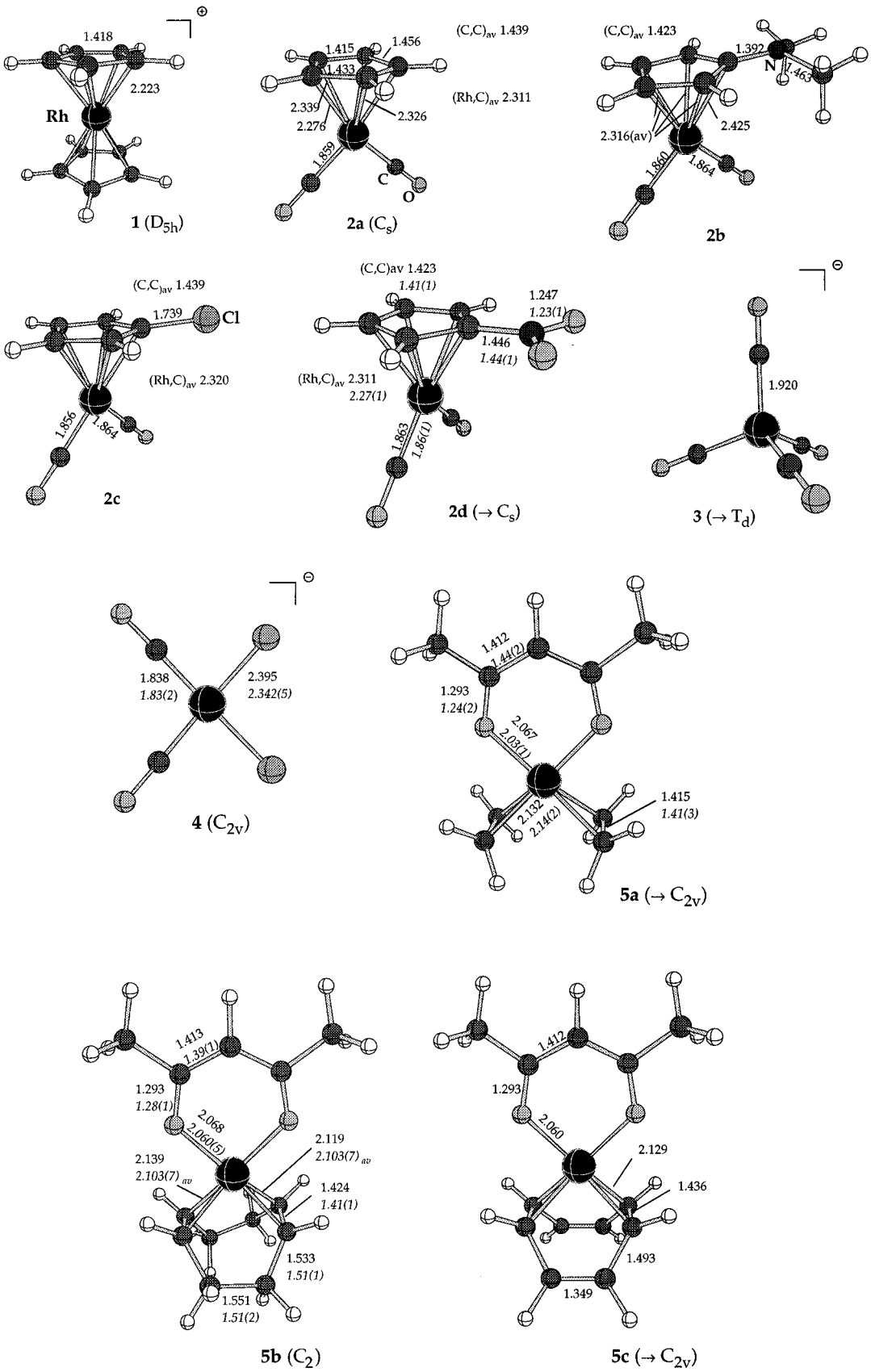

Figure 1. BP86/ECP1 optimized geometries of compounds **1**−**5** (C_1 symmetry except where indicated; → indicates that the optimization started from a lower symmetry). Important bond lengths (Å) are included, together with the corresponding, averaged data (*in italics*) from the following crystal structure determinations: **2d**,[55] **4**,[56] **5a**,[57] and **5c**.[58]

key geometrical parameters and experimental, X-ray-derived values where available. In general, the optimized bond distances tend to be somewhat longer than found in the solid state[55−58] but are mostly within the experimental uncertainties (taken as 3σ), which are fairly large in most cases. For consistency, the theoretical geometries have been employed in the chemical shift calculations.

Table 1. Absolute Magnetic Shieldings σ and Relative Chemical Shifts δ for ^{103}Rh in Organorhodium Compounds 1−5, Computed with the GIAO-SCF and SOS-DFPT Methods[a]

	σ(calcd)			δ(calcd)[c]				
compd[b]	SCF/IIa	DFPT/II	DFPT/IIa	SCF/IIa	DFPT/II	DFPT/IIa	DFPT/IIa (scaled)[d]	δ(exptl)[e]
$[Rh(C_5H_5)_2]^+$ (**1**)	−713.3	1251.8	1231.6	−1829	−1581	−1614	−2069	−1839
$[Rh(CO)_2(C_5H_5)]$ (**2a**)	−780.9	697.6	643.8	−1761	−1027	−1026	−1315	−1322
$[Rh(CO)_2(C_5H_4NMe_2)]$ (**2b**)	−877.6	562.0	521.1	−1665	−892	−904	−1159	−1248
$[Rh(CO)_2(C_5H_4Cl)]$ (**2c**)	−989.7	530.4	493.8	−1553	−860	−876	−1123	−1166
$[Rh(CO)_2(C_5H_4NO_2)]$ (**2d**)	−969.0	541.1	495.5	−1573	−871	−878	−1126	−1117
$[Rh(CO)_4]^-$ (**3**)	−788.0	305.7	141.7	−1754	−635	−524	−672	−644
cis-$[RhCl_2(CO)_2]^-$ (**4**)	−2334.7	−597.2	−676.4	−208	268	294	377	84
$[Rh(acac)(C_2H_4)_2]$ (**5a**)	−4343.9	−1140.7	−1177.4	1802	811	795	1019	1184
[Rh(acac)(COD)] (**5b**)	−4507.8	−1386.0	−1418.5	1966	1057	1036	1328	1306
[Rh(acac)(COT)] (**5c**)	−5051.9	−1696.8	−1728.2	2510	1367	1346	1726	1760
slope[f]	−1.36	−0.79	−0.78					
intercept[f]	−2524.3	−329.5	−382.6					
mean abs dev from expt				497	267	280	92	

[a] In ppm; BP86/ECP1 geometries employed. [b] Abbreviations: acac = acetylacetonato, COD = 1,5-cyclooctadiene, COT = cyclooctatetraene. [c] Relative to the intercepts at δ 0 of the σ(calcd)/δ(exptl) linear regressions (values in the next to last row). [d] DFPT/IIa results, scaled with 1/0.78. [e] From refs 5, 49, and 50. [f] From σ(calcd)/δ(exptl) linear regressions.

The computed SOS-DFPT results are summarized in Table 1, together with the corresponding SCF values (for comparison) and the experimental data, and are plotted in Figure 2.

As expected, the classical GIAO (gauge-including atomic orbitals)-SCF method does not afford a good description of the ^{103}Rh chemical shifts and gives erratic results in some cases (see Figure 2a). Nevertheless, trends in closely related systems such as **2a**−**d** or **5a**−**c** are reproduced qualitatively. The substituent effects on $\delta(^{103}Rh)$, however, are substantially overestimated at the SCF level, as judged by the slope of the linear regression line, 1.36 (Table 1). The correlation between experimental and theoretical $\delta(^{103}Rh)$ data is noticeably improved at the SOS-DFPT/IIa level (Figure 2b), but the slope of this regression line is only 0.78 instead of unity. As in the case of $\delta(^{57}Fe)$,[29] substituent effects on the metal chemical shift are underestimated with the SOS-DFPT approach, but less drastically so for $\delta(^{103}Rh)$ than for $\delta(^{57}Fe)$. In the present study, no particular problem case is evident for the theoretical ^{103}Rh chemical shifts. In contrast, $\delta(^{57}Fe)$ of ferrocene, the analogue of **1**,[59] deviates substantially from the σ(calcd)/δ(exptl) correlation at the same theoretical level.[29]

Basis set effects do not seem to affect the SOS-DFPT chemical shifts significantly: basically the same slope of the σ(calcd)/δ(expt) regression line is obtained when basis II is used, i.e. a somewhat smaller basis on Rh (Table 1). For **1** and **5c**, the "extremes" of the test set, additional SOS-DFPT calculations have been performed employing a larger basis set on the ligands, as well as various local or nonlocal density functionals (see Computational Details). In no case has the computed difference of the magnetic shieldings, i.e. the chemical shift range covered, differed notably from the SOS-DFPT/IIa value.

No relativistic effects are incorporated in the present model. It is unlikely, however, that relativity will affect the relative ^{103}Rh chemical shifts drastically. Changes in $\delta(^{103}Rh)$ due to relativistic effects are probably smaller than other possible errors. Trends in $\delta(^{91}Zr)$, another 4d transition metal, are well-reproduced at nonrelativistic theoretical levels,[60] and scalar relativistic

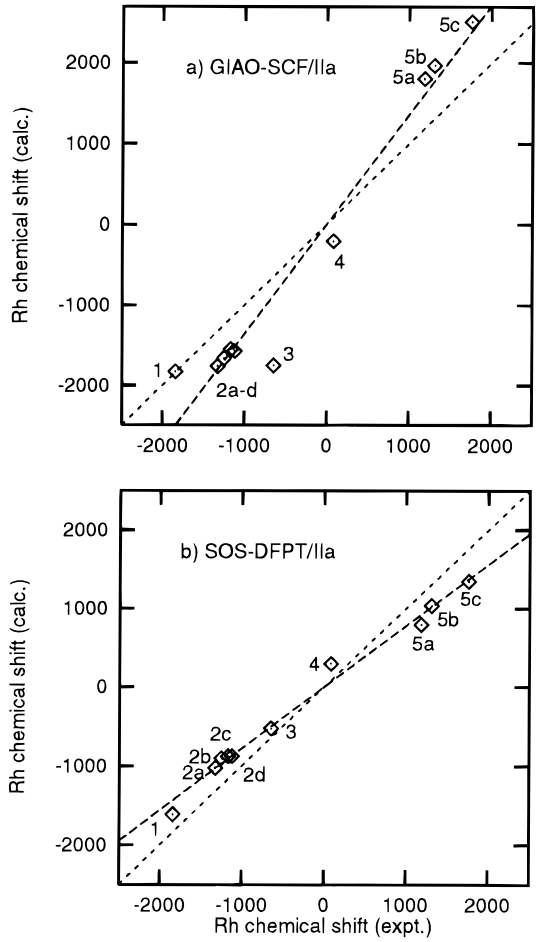

Figure 2. Plots of computed (basis II for BP86/ECP1 optimized geometries) vs experimental ^{103}Rh chemical shifts: (a) GIAO-SCF level; (b) SOS-DFPT level. Linear regression lines (dashed) and ideal lines with the slope 1 (dotted) are included.

(55) Rausch, M. D.; Hart, W. P.; Atwood, J. L.; Zaworotko, M. J. *J. Organomet. Chem.* **1980**, *197*, 225.
(56) Mantovani, A.; Pelloso, M.; Bandoli, G.; Crociani, B. *J. Chem. Soc., Dalton Trans.* **1984**, 2223.
(57) Evans, J. A.; Russell, D. R. *J. Chem. Soc. D* **1971**, 197.
(58) Tucker, P. A.; Scutcher, W.; Russell, D. R. *Acta Crystallogr.* **1975**, *B31*, 592.
(59) Like ferrocene, isolated **1** is computed to adopt an eclipsed conformation; the staggered D_{5d} form is 0.3 kcal/mol higher in energy at the BP86/ECP1 level.
(60) Bühl, M.; Hopp, G.; von Philipsborn, W.; Beck, S.; Prosenc, M.-H.; Rief, U.; Brintzinger, H.-H. *Organometallics* **1996**, *15*, 778.

effects on the metal chemical shift of $Mo(CO)_6$ have been shown to be rather small.[61]

The reasons for the apparent shortcomings of the density functionals used are presently unclear. Given the over- and underestimation of $\delta(^{103}Rh)$ at SCF and DFT levels, respectively, one might speculate if so-called hybrid functionals,[53] which include certain amounts of Hartree−Fock (SCF) exchange, could improve the theoretical $\delta(^{103}Rh)$ chemical shift range.[70]

Concerning practical applications, the correlation in Figure 2b suggests that an appropriate scaling of the present theoretical $\delta(^{103}Rh)$ values could afford reasonably accurate calculated chemical shifts. It is not uncommon to scale ab initio results, e.g. in the case of energies[62,63] or vibrational frequencies;[34] also, the scaling of GIAO-SCF computed ^1H chemical shifts has been proposed recently.[64] The accord between the scaled SOS-DFPT/IIa data and the experimental ^{103}Rh chemical shifts is indeed noteworthy (compare the last two entries in Table 1). For the present set of compounds, the mean absolute deviation between calculated and experimental chemical shifts is only 92 ppm, i.e. less than 3% of the chemical shift range covered. In view of the pronounced dependencies of $\delta(^{103}Rh)$ values on factors such as solvent and temperature,[49,50] this degree of agreement would appear satisfactory. The theoretical chemical shifts of substances where no experimental $\delta(^{103}Rh)$ data are available should be of useful, predictive value.

The qualitative trend in $\delta(^{103}Rh)$ for **2a**−**d**, the reactants in the displacement reaction (1), is well-reproduced computationally, in particular the deshielding in going from **2a** (X = H) to **2b** (X = NMe_2) or **2d** (X = NO_2). Since the NMe_2 group is a strong π-donor, the overall electron density in the cyclopentadienyl−Rh moiety of **2b** should increase with respect to the parent **2a**, and an increased shielding of $\delta(^{103}Rh)$ might have been expected. The observed deshielding has led to the postulation of a resonance effect toward a "ring-slipped" η^3 species (see also below), either "in the ground state or in a low-lying electronically excited state".[5] No bond length changes indicative of such a resonance effect are apparent in the DFT-optimized geometries of **2a** and **2b**: the computed variations of the C−C bond lengths, up to ca. 4 pm, are practically the same for both molecules. The most pronounced geometrical change in going from **2a** to **2b** is the increase of the Rh−C(ipso) distance from 2.28 to 2.42 Å (see Figure 1). This trend toward reduced coordination of the rhodium atom is consistent with the observed deshielding of the ^{103}Rh nucleus.

The SOS-DFPT calculations are performed in an IGLO framework (individual gauge for localized orbitals),[36−38] which permits the breakdown of the computed shielding tensor σ into contributions from localized MOs. Unfortunately, no systematic changes of the individual contributions are found in the series **2a**−**d**, nor can the trend in σ be attributed to a single or a few MOs. It is interesting to note, however, that a large fraction (ca. 80 ppm) of the deshielding of **2b** with respect to **2a** indeed stems from increased paramagnetic contributions of the cyclopentadienyl "π"-MOs (localized on the same side as Rh). Thus, the postulated resonance effects may indeed play a role. In this context photolectron spectra have been used to assess the relative inductive and resonance effects of the substituents at the cyclopentadienyl ring.[65]

Scheme 1

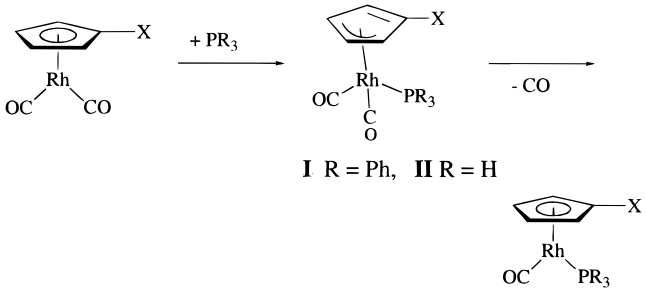

2. Reactivities. From the rate law and from small, negative entropies of activation, an associative mechanism has been deduced for the CO/PPh_3 displacement reaction (1).[66,67] In order to accommodate the incoming phosphine ligand, a "ring slipping" from the η^5- to a η^3-cyclopentadienyl species has been inferred for the transient adduct **I** (cf. Scheme 1). Support for this mechanism comes from the unusually high reactivity of the corresponding η^5-indenyl complexes, consistent with the expected gain in resonance energy in the attached six-membered ring.[68]

The pathway leading to such a η^3-ring-slipped adduct has now been studied for the reaction of the parent **2a** with PH_3 as model phosphine. At the BP86/ECP1 level, the adduct **IIa** is a true minimum on the potential energy surface (PES) and is 14.5 kcal/mol above the reactants. The transition state **IIa(TS)** for formation of the intermediate **IIa** is only 1 kcal/mol above the latter, affording an activation barrier ΔE_a of 15.5 kcal/mol, in good agreement with the experimental $\Delta H^{\ddagger}$ data (estimated ca. 15 kcal/mol for R = OC_4H_9).[66] The PES is quite flat in the region of the transition state: the 1 kcal/mol increase in energy in going from **IIa** to **IIa-(TS)** is paralleled by an elongation of the Rh−P distance of nearly 0.3 Å (see Figure 3).

However, PH_3 is not a good model for the phosphines used experimentally. Since PH_3 forms weaker complexes than CO, reaction 1 (X, R = H) is computed to be strongly endothermic, by 17.5 kcal/mol (cf. the schematic pathway in Figure 3). With the phosphines used in practice, the products will be similar to or lower in energy than the reactants. It is thus probably safe to assume that the activation barrier for CO loss from **I** will be as low as the barrier for phosphine loss and that formation of the intermediate **I** is the rate-determining step. The quantitative results for the models **II** involving PH_3 might be of limited use, but the relative trend brought about by the substituents should be comparable for systems **I** and **II**.

(61) Schreckenbach, G.; Ziegler, T. *Int. J. Quantum Chem.*, in press.
(62) Siegbahn, P. E. M.; Svensson, M.; Boussard, P. J. E. *J. Chem. Phys.* **1995**, *102*, 5377.
(63) Siegbahn, P. E. M.; Blomberg, M. R. A.; Svensson, M. *Chem. Phys. Lett.* **1994**, *233*, 35.
(64) Chesnut, D. B. In *Reviews in Computational Chemistry*; Lipkowitz, K. B., Boyd, D. B., Eds.; VCH: New York, 1996; Vol. 8, p 245.
(65) Lichtenberger, D. L.; Renshaw, S. K.; Basolo, F.; Cheong, M. *Organometallics* **1991**, *10*, 148.
(66) Chong, M.; Basolo, F. *Organometallics* **1988**, *7*, 2041.
(67) Schuster-Woldan, H. G.; Basolo, F. *J. Am. Chem. Soc.* **1966**, *88*, 1675.
(68) Li, L.-N.; Rerek, M. E.; Basolo, F. *Organometallics* **1984**, *3*, 740.

Table 2. Absolute (au) and Relative (kcal/mol, in Parentheses) Single-Point Energies[a] for the Stationary Points of the CO/PH_3 Displacement Reaction of 2a

level[a]	**2a** + PH_3			**IIa(TS)**		**IIa**		$[Rh(C_5H_5)(PH_3)(CO)]$ + CO		
SCF	−527.415 21	−342.444 60	(0.0)	−869.818 26	(26.1)	−869.812 21	(29.9)	−757.122 00	−112.733 97	(2.4)
VWN	−528.688 85	−342.168 53	(0.0)	−870.842 34	(9.4)	−870.847 99	(5.9)	−758.142 65	−112.683 40	(19.7)
B3LYP	−530.832 62	−343.137 59	(0.0)	−873.941 61	(17.9)	−873.940 85	(18.4)	−760.640 25	−113.306 58	(14.7)
BPW91	−530.881 47	−343.125 05	(0.0)	−873.979 93	(16.7)	−873.981 18	(15.9)	−760.683 22	−113.296 01	(17.1)
BP86	−530.939 55	−343.152 27	(0.0)	−874.067 10	(15.5)	−874.068 74	(14.5)	−760.758 81	−113.305 20	(17.5)

[a] Employing ECP1 basis and BP86/ECP1 geometries.

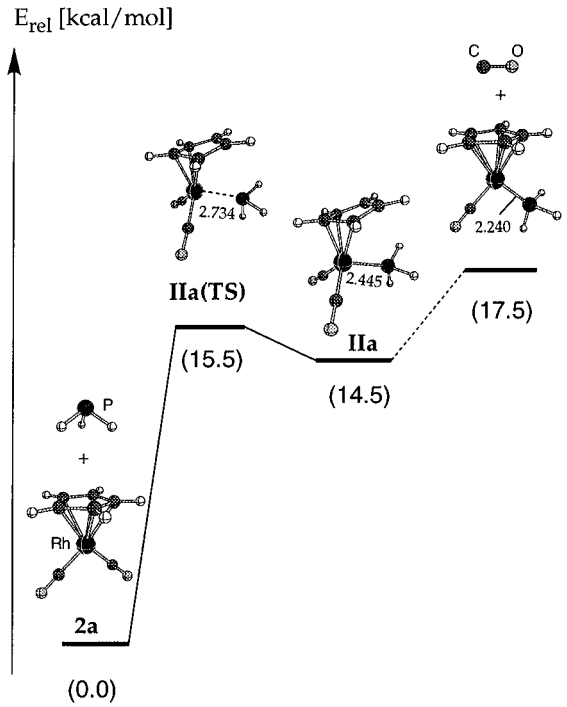

Figure 3. Schematic reaction profile for PH_3 addition to **2a** (BP86/ECP1 level). The transition structure for the CO dissociation (dotted path) has not been calculated (see text).

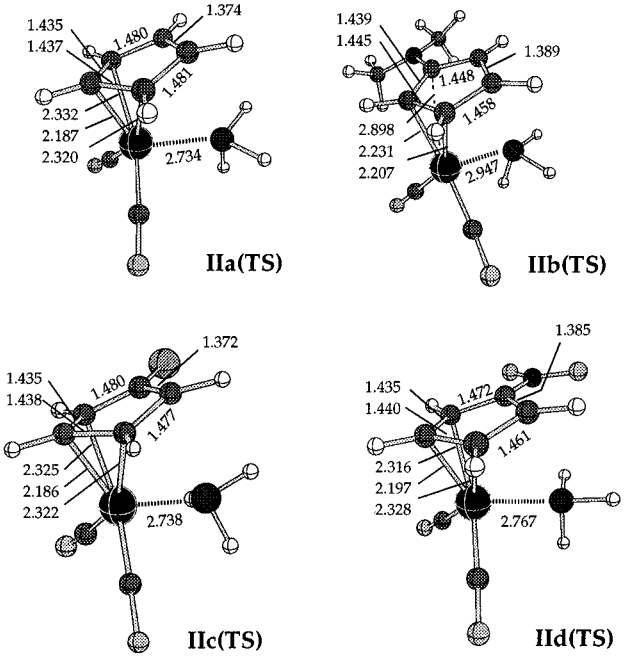

Figure 4. Transition structures **IIa(TS)**−**IId(TS)** for PH_3 addition to **2a**−**d** (BP86/ECP1 optimized).

Table 3. Experimental Kinetic Data[a] and Computed Activation Energies[b] for the CO/PR_3 Displacement Reaction (1)

X	k_{obsd} (M^{-1} s^{-1})	k_{rel}	ΔE_a (kcal/mol)
H	1.30×10^{-4}	1	15.5
NMe_2	1.05×10^{-3}	8	12.0
Cl	5.18×10^{-2}	40	11.1
NO_2	1.26	9700	9.6

[a] For CO/PPh_3 displacement; from ref 66. [b] For addition of the model phosphine PH_3, BP86/ECP1 level.

In order to test if the qualitative aspects of this reaction depend on the specific functional used, additional single-point energy calculations have been performed for the BP86/ECP1 geometries. The results in Table 2 indicate that, at the SCF and the B3LYP levels, the transition state **IIa(TS)** may well disappear and **IIa** may become the actual transition structure, as the former is computed to be more stable than the latter at these levels. Thus, a definitive conclusion regarding the nature of the transient species **I** (transition state or intermediate) cannot be given yet. In any case, as pointed out above, the PES is quite flat in the region of the transition state.

Consistent with the general performance of the respective theoretical methods, the overall barrier is too large at the SCF level (ca. 30 kcal/mol, Table 2) and is too low with the local density approximation (cf. VWN value in Table 2, ca. 9 kcal/mol). The "pure DFT" combinations BP86 and BPW91 give very similar results, and the former method has been employed for the further study of effects of derivatization at the cyclopentadienyl moiety.

The substituted transition states **IIb(TS)**−**IId(TS)** have been located and are displayed in Figure 4, together with the parent **IIa(TS)**. Except for **IIb(TS)**, they are all characterized by a η^3-cyclopentadienyl ligand, showing an essentially uncoordinated "double bond" with a C−C bond length around ca. 1.37 Å, which bears the substituent. In contrast, the NMe_2 rest in **IIb(TS)** is placed in a position α to the "double bond", and the hapticity of the cyclopentadienyl moiety is further reduced toward η^2. This result is quite surprising, since the corresponding NH_2 analog shows the same characteristics as **IIc(TS)** and **IId(TS)**. Despite the different transition structures, the barriers for X = NMe_2 and X = NH_2 are quite similar (within 2 kcal/mol). Apparently, the location of the NR_2 group at either the η^3-coordinated or at the noncoordinated part of the cyclopentadienyl ligand is delicately balanced and may perhaps depend on the theoretical level employed. The energetic preference for either position appears to be small, and the following, qualitative energetic arguments should not be affected.

The computed activation barriers ΔE_a of PH_3 addition to **2a**−**d** are collected in Table 3, together with the experimental rate constants for CO/PPh_3 displacement. Both sets of data correlate well; the increase in the experimental rates of nearly 5 orders of magnitude is

Scheme 2

minima:

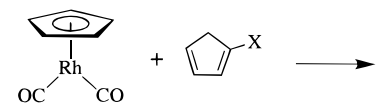

X	ΔE [kcal/mol]
NMe_2	+0.3
Cl	+4.9
NO_2	+4.9

transition states:

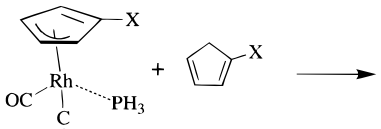

X	ΔE [kcal/mol]
NMe_2	-3.8
Cl	+0.5
NO_2	-1.0

paralleled by a decrease in the computed ΔE_a of 5.9 kcal/mol, consistent with estimates from simple transition state theory[69] assuming constant preexponential factors. A more detailed analysis of the dynamics of the systems would probably be needed for definitive conclusions, but it appears that the lowering of the free energy of activation in this system is immediately related to the decrease of ΔE_a in the respective potential energy surfaces.

The isodesmic equations summarized in Scheme 2 may serve to estimate the energetic effects brought about by replacement of a H atom by the various substituents X in **2a** or in **IIa(TS)**. Consistent with the variations in the transition state geometries discussed above, the substituents affect ΔE_a in different ways: while the electron-withdrawing groups Cl and NO_2 are indicated to lower the barrier by destabilizing the minima with respect to **2a**, the electron-donating NMe_2 group does so by stabilizing the transition state with respect to **IIa(TS)**.

Both the trends in $\delta(^{103}Rh)$ and in the kinetic parameters observed for **2a**−**d** are thus reproduced theoretically. However, no definitive answer can be given yet regarding the intrinsic relation between these two properties, mainly because the variation in $\delta(^{103}Rh)$ is rather small (compared to the total chemical shift range) and does not lend itself to a straightforward interpretation in the theoretical framework used (see end of chemical shift section). Other systems are currently under study which are more promising in that respect.

(69) Benson, S. W. *Thermochemical Kinetics*; Wiley: New York, 1976.

Conclusion

In summary, experimental ^{103}Rh chemical shifts of a number of organorhodium complexes can be well-reproduced with the SOS-DFPT method, but only after appropriate scaling. Without scaling, only ca. 80% of the substituents on $\delta(^{103}Rh)$ are recovered in the calculations, as judged from the slope of the σ(calcd) vs δ(expt) correlation. Nevertheless, these results offer for the first time the prospect of a reliable theoretical prediction of trends in $\delta(^{103}Rh)$,[70] opening numerous possibilities for future applications.

The model CO/PH_3 displacement reaction in [Rh(C_5H_5)$(CO)_2$] (**2**) is shown to proceed via a "ring-slipped" η^3 intermediate, as deduced experimentally for the reaction with substituted phosphines. The computed activation barriers for PH_3 addition to **2a**−**d** can be correlated with the experimental rate constants for CO/PPh_3 displacement. Thus, the empirical correlation between the kinetic parameters of these complexes with their $\delta(^{103}Rh)$ values is reproduced theoretically and the approach described here appears well-suited for the further study of such NMR/reactivity correlations.

Acknowledgment. I wish to thank Prof. Dr. W. Thiel and the Fonds der Chemischen Industrie for support. The assistance of O. L. Malkina and Dr. V. G. Malkin with deMon is gratefully acknowledged. Discussions with Dr. U. Fleischer, Dr. M. Kaupp, Dr. W. Leitner, and Prof. W. von Philipsborn have been very helpful. The calculations have been carried out on a Silicon Graphics PowerChallenge and on IBM RS6000 workstations at the University of Zürich and at the ETH Zürich (C4 cluster), as well as on the NEC-SX3 at the CSCS in Manno, Switzerland.

Supporting Information Available: A listing of Gaussian 94 archive entries of the BP/ECP1 optimized geometries (7 pages). Ordering information is given on any current masthead page.

OM960615Y

(70) After the initial submission of this paper it has been found that not only ^{103}Rh but also ^{57}Fe chemical shifts are in fact well-described without scaling at the GIAO-B3LYP level; see: Bühl, M. *Chem. Phys. Lett.*, submitted for publication.